Functional Nanoparticles

DOI: 10.1002/anie.201007847

Bifunctional Hybrid SiO_2 Nanoparticles Showing Synergy between Core Spin Crossover and Shell Luminescence Properties**

Silvia Titos-Padilla, Juan Manuel Herrera, Xiao-Wei Chen, Juan José Delgado, and Enrique Colacio**

It is well-known that certain octahedral coordination compounds with electronic configurations from d^4 to d^7 can undergo spin crossover (SCO) between high-spin (HS) and low-spin (LS) states.[1] The spin state, and consequently the color, size, and magnetic properties of these SCO systems can be tuned through external stimuli such as temperature, pressure, light, magnetic fields, and guest absorption/desorption.[2] Additionally, some SCO compounds exhibit abrupt transitions with large hysteresis loops, which confer a memory effect to these materials. Therefore, SCO systems offer some promising opportunities for application in information processing, data storage, molecular switches, and/or display devices.[3] For integration into functional devices, SCO materials need to be prepared at the nanometer scale, whilst retaining their magnetic and cooperative behavior. As a result, different research groups have focused their studies on the synthesis and physicochemical characterization of spin-crossover nanoparticles (SCONPs). They have demonstrated that the SCO phenomenon is preserved at the nanometer scale and that it is possible to tune the transition temperatures and the size of the hysteresis loop by controlling the particle size.[4]

Parallel to this approach, some other research groups have concentrated their studies on the design of new molecular systems that combine spin crossover and other interesting properties such as luminescence.[5] To the best of our knowledge, only one attempt has been made to prepare bifunctional SCO/luminescence nanoparticles. Specifically, Bousseksou and co-workers[6] have obtained nanoparticles of the SCO complex $[Fe(NH_2Trz)_3](tos)_2$ (NH_2Trz = 4-amino-1,2,4-triazole; tos = tosyl) doped with the fluorescent agent Rhodamine 110. In this system, the emission spectrum of the Rhodamine at room temperature overlaps with the $^1A_{1g}\rightarrow{}^1T_{1g}$ absorption band of the iron(II) polymer in the LS state and the emission is partially quenched. When the temperature is raised to 320 K (HS regime), the $^1A_{1g}\rightarrow{}^1T_{1g}$ absorption band bleaches and the emission intensity increases.

Herein, we propose an alternative strategy to prepare bifunctional SCO/luminescence nanoparticles which consists of using silica as a matrix for the SCO component (Figure 1). Although silica nanoparticles (SiO_2NPs) have been widely used as supports for the fabrication of multifunctional materials that have a vast number of important potential applications in fields such as drug delivery, biosensors, cell labeling, and so forth,[7] as far as we know, no examples of hybrid SiO_2NPs⊃SCO systems have been reported so far. Silica is a particularly suitable material for the preparation of SiO_2NPs⊃SCO systems because its high porosity allows for the incorporation of SCO compounds and as silica does not absorb light and does not interfere with magnetic fields the SCO compounds inside the SiO_2NPs will keep their original optical and magnetic properties. Additionally, the surfaces of these SiO_2NPs⊃SCO systems can be functionalized by grafting active species, such as fluorophores, to afford bifunctional SCO/luminescence nanomaterials.

The first results of this original approach are reported, herein. As the SCO material we have used a 1D Fe^{II} complex $\{[Fe(HTrz)_2(Trz)](BF_4)\}_n$ (hereafter Fe-Trz; HTrz = 1,2,4-1*H*-

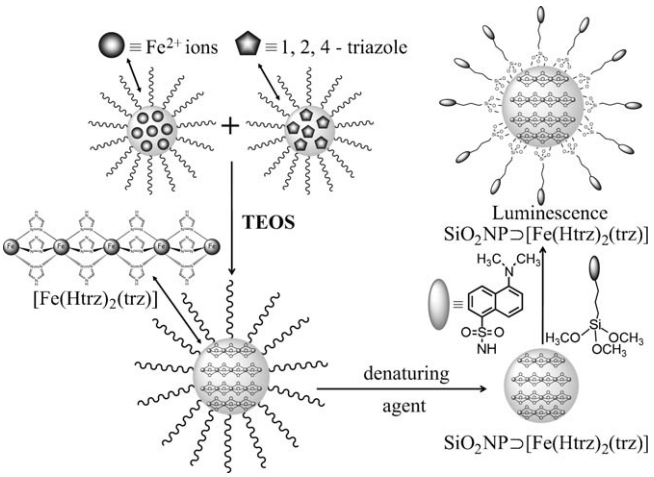

Figure 1. Synthetic route and schematic representation of the SCO/luminescence SiO_2NPs.

[*] S. Titos-Padilla, Dr. J. M. Herrera, Prof. E. Colacio
Departamento de Química Inorgánica
Facultad de Ciencias, Universidad de Granada
Avda. Fuentenueva s/n, 18071, Granada (Spain)
Fax: (+34) 95-824-8526
E-mail: jmherrera@ugr.es
ecolacio@ugr.es
X.-W. Chen, Dr. J. J. Delgado
Departamento de Ciencia de los Materiales
e Ingeniería Metalúrgica y Química Inorgánica
Facultad de Ciencias, Universidad de Cádiz
11510, Puerto Real, Cádiz (Spain)

[**] Financial support from the Spanish Ministerio de Ciencia e Innovación (MICINN) (CTQ-2008-02269/BQU), the Junta de Andalucia (FQM-195, the Project of excellence P08-FQM-03705), and the University of Granada (research contract to J.M.H.) is acknowledged. S.T.-P. thanks the Junta de Andalucia for a research grant. We are also grateful to Prof. Fermín Capitán and Sonia Capel for their continuous and generous assistance with the temperature-dependent luminescence experiments.

Supporting information for this article is available on the WWW under http://dx.doi.org/10.1002/anie.201007847.

triazole) that exhibits an abrupt transition with large thermal hysteresis centered close to room temperature.[8] As the fluorophore we have used 3-(dansylamido)propyltrimethoxysilane (hereafter, dansyl) which was grafted on the surface of the SiO_2⊃Fe-Trz. Hybrid SiO_2NPs⊃Fe-Trz samples have been prepared by using the well-established reverse micelle technique (see the Experimental Section).[9] Hybrid **1** was obtained as a purple solid at room temperature from an aqueous 0.625 M solution of iron(II) ions and a stoichiometric amount of the HTrz ligand. To test the effect of the Zn^{II} doping on the magnetic properties of the nanoparticles hybrid SiO_2NPs⊃Fe/Zn-Trz has been prepared with polymers of the type $\{[Fe_{1-x}Zn_x(HTrz)_2(Trz)](BF_4)\}_n$. Hybrids **2** and **3** were synthesized by the same procedure as for **1,** but with different Fe/Zn ratios, 0.8:0.2 for **2** and 0.5:0.5 for **3**. In both cases, the concentration of the metallic ions in water, $c(Fe^{II}) + c(Zn^{II})$, was kept constant and equal to 0.625 M. Finally, the surfaces of **1** and **3** were functionalized with the organic fluorophore 3-(dansylamido)propyltrimethoxysilane to yield **1-dansyl** and **3-dansyl**, respectively.

TEM and high-angle annular dark-field-scanning transmission electron microscopy (HAADF-STEM) images of **1** are shown in Figure 2. The nanoparticles, which are fairly monodisperse and well-defined, show a rodlike topology with an average side length and width of (147 ± 11.7) and (92.1 ± 12.1) nm, respectively. To determine the inclusion of the iron polymer into the silica matrix, energy dispersive X-ray spectroscopy (EDX) experiments were performed, which showed the juxtaposition of the Fe^{II} polymer and the silica matrix. Post-acquisition data analysis leads to two images that map the spatial distribution of the Si and Fe atoms with a brighter contrast corresponding to a high concentration of one of these two elements. The line profile obtained by EDX analysis clearly indicates that the iron polymer is 1) fully incorporated into the nanoparticles and 2) surrounded by a narrow outer shell of pure silica (see Figure S6 in the Supporting Information).

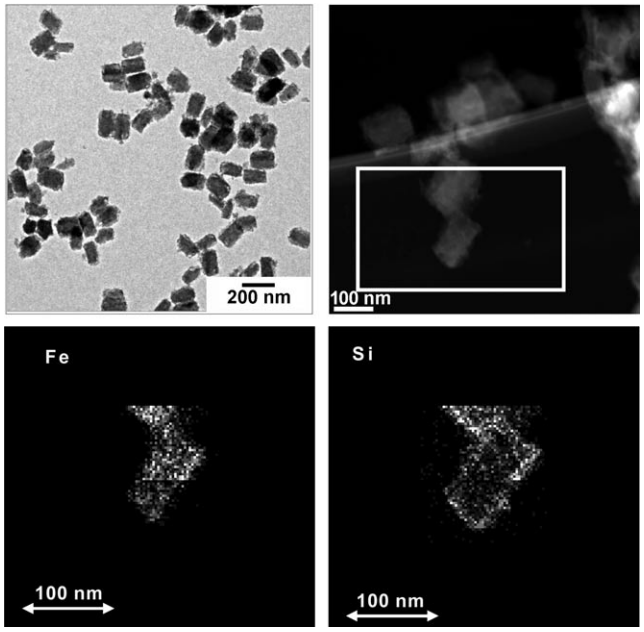

Figure 2. TEM (top left) and HAADF-STEM (top right) images of **3**. EDX compositional maps of Fe (bottom left) and Si (bottom right) were collected from the square area indicated on the HAADF-STEM image.

TEM images of **2** and **3** (see Figures S2 and S3 in the Supporting Information) show how the doping the SCO polymer with Zn^{II} ions induces significant changes in the shape and size of the nanoparticles. Hybrid **2** appears as rectangular prisms with dimensions of (142.8 ± 16.1) nm in length and (51.2 ± 9.0) nm in width. The nanoparticles are similar in length as in **1**, but significantly narrower. The structural changes become more significant as the ratio of Zn^{II} ions increases. Thus in **3**, the length of the nanoparticles increases up to (188.9 ± 37.4) nm whereas the width decreases to (28.8 ± 7.1) nm. At the moment, we do not know the origins of the rodlike shape of the SiO_2NPs⊃Fe-Trz and the size and shape changes they undergo when the ratio of Zn^{II} ions increases. These aspects are the subject of a further study. Compositional mapping of **3** by EDX indicates that the Fe^{II} and Zn^{II} ions are randomly distributed in the silica matrix. Even though the global ratio Fe/Zn, which was found in large areas of the sample, is close to 1:1 as expected, the distribution of the Fe^{II} and Zn^{II} ions within the nanoparticle is not completely homogeneous. At some sites the iron (zinc) ions are the major species within the sample.

TEM images of **1-dansyl** and **3-dansyl** (see Figures S4 and S5 in the Supporting Information) reveal that the shape and size of the nanoparticles are not significantly modified when the dansyl fluorophore is grafted through an alkoxysilane group onto their surface. Nevertheless, significant particle aggregation is observed. This fact is usually observed for post-coated silica nanoparticles with organosilane groups. Silica nanoparticles are usually well-dispersed and non-aggregated as a result of repulsive forces promoted by the strong negative charge on their surface, which stems from the deprotonated silanol groups (Si–OH→Si–O^-). The organosilane groups grafted onto the surface of the nanoparticles neutralize these negative charges, which leads to a decrease of the colloidal stability and then to particle aggregation.[7c] The EDX compositional maps of **1-dansyl** indicate a quite homogeneous distribution of Fe and Si atoms within the nanoparticles. In addition, a sulfur signal is detected which corresponds to covalent attachment of the dansyl groups on the surface of the nanoparticles through the alkoxysilane groups.

A comparison of the powder X-ray diffraction pattern of the bulk material with those of compounds **1–3** (Figure S9 in the Supporting Information) reveals that the coordination polymers embedded within the silica matrix (amorphous) are isostructural to the bulk material.

The thermal dependence of $\chi_M T$, in which χ_M is the molar magnetic susceptibility and T is the temperature, for **1–3** (Figure 3) was measured with a heating and cooling sweep rate of 10 K min^{-1}. The SCO phenomenon is clearly preserved in each sample. The spin transition in **1** remains similar to that reported for the bulk sample. At 400 K, the $\chi_M T$ value of 3.48 $cm^3 K mol^{-1}$ fits well with the expected value for an iron(II) ion in the HS state. The spin transition is very abrupt and shows a well-shaped thermal hysteresis loop of more than 40 K. As expected, the doping with Zn^{II} ions leads to important changes in the magnetic properties of the hybrid

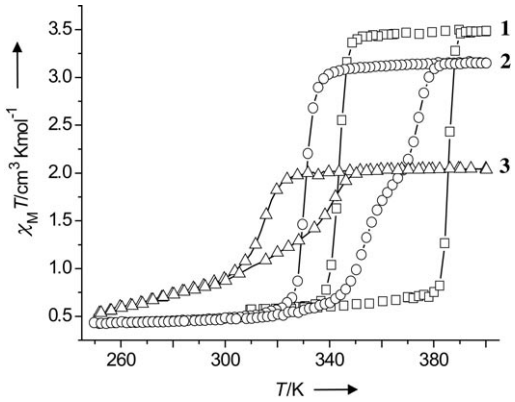

Figure 3. Plots of $\chi_M T$ versus T for **1** (open squares), **2** (open circles), and **3** (open triangles).

nanoparticles. As the ratio of Zn^{II} ions increases, the transition is less abrupt, it moves to lower temperatures, and the thermal hysteresis becomes narrower. The increase in the magnetic moment of **2** during the heating protocol is quite smooth between 345 and 370 K and then it comes to abrupt saturation. The spin crossover takes place by a two-step process with $T_C\uparrow = 353$ and 374 K, respectively. Conversely, in the cooling process, the entire transition is sharp with $T_C\downarrow =$ 330 K. This behavior has previously been observed in other nanoparticles formed by Fe/Zn-triazole polymers, and it has been related to the random distribution of Zn^{II} ions along the chains. The diamagnetic Zn^{II} ions shorten the length of the Fe-Trz chains and interrupt the cooperativity effects in a random way, which ultimately leads to a significant change in the hysteresis loop.[4a,h] This hypothesis agrees with the non-homogeneous distribution of the Fe^{II} and Zn^{II} ions observed in this sample by EDX analysis. For **3**, the transition is quite smooth in both the heating and cooling protocols with $T_C\uparrow =$ 342 K, $T_C\downarrow = 316$ K, and with a thermal hysteresis with a width of 26 K. The spin transition is also observed for **1-dansyl** and **3-dansyl** (see Figure S10 in the Supporting Information). The shapes of the hysteresis loops are similar to those shown by **1** and **3**, although their width and critical temperatures vary slightly (**1-dansyl**: $T_C\uparrow = 392$ K, $T_C\downarrow = 343$ K, $\Delta T = 49$ K; **3-dansyl**: $T_C\uparrow = 363$ K, $T_C\downarrow = 328$ K, $\Delta T = 35$ K).

In the bulk phase, the LS→HS transition is accompanied by a noticeable change of color, from pink-violet (LS state) to white (HS state). The same thermochromic behavior is observed for **1–3** (see Figure S11 in the Supporting Information). The diffuse reflectivity spectra at 280 K of **1–3** display two absorption bands centered at 538 and 382 nm, which are characteristic of the d–d transitions in the LS state ($^1A_{1g}\rightarrow{}^1T_{1g}$ and $^1A_{1g}\rightarrow{}^1T_{2g}$). These bands completely vanish at 400 K,, which confirms the HS configuration of the Fe^{II} ions at this temperature. The d–d transition of the HS state ($^5T_{2g}\rightarrow{}^5E_g$) is expected to appear at lower energy in the near-infrared region.

After irradiation at 315 nm, **1-dansyl** and **3-dansyl** display a broad fluorescence band centered at approximately 495 nm, which is typical for dansyl groups.[10] In contrast to the expected thermal quenching of the fluorescence (as a result of thermal population of non-emitting excited states), the emission intensity at 400 K (HS regime) is up to three times more intense than that observed for **1-dansyl** at 280 K (LS regime) and close to double that of **3-dansyl**. If the absorption and emission spectra of these samples are compared, one immediately realizes that fluorescence becomes more intense when the LS absorption band $^1A_{1g}\rightarrow{}^1T_{1g}$ at 538 nm is bleached. The thermal variation of the fluorescence intensity at 494 nm of **3-dansyl** in the 283–373 K range (Figure 4b) is almost identical in shape to the observed thermal dependence of the $\chi_M T$ product (Figure S10b in the Supporting Information). The critical temperatures obtained from the thermal variation of the luminescence are 357 and 323 K in the heating and cooling modes, respectively. Therefore, it appears that the changes in the fluorescence intensity are synchronized with the thermally induced SCO transition. The quenching of the dansyl fluorescence by the Fe^{II}-LS complex can be ascribed to an energy transfer from the dansyl group to the LS complex since there exists a reasonable spectral overlap between the dansyl fluorescence and the LS absorption band $^1A_{1g}\rightarrow{}^1T_{1g}$ of the iron(II) ion. The different degree of quenching for **1-dansyl** and **3-dansyl** is related to the Fe^{II}/dansyl ratio in the two samples. Thus, an increase in the Fe^{II}/dansyl ratio increases the quenching.

In summary, we have designed hybrid SiO_2NPs with a SCO-polymer core and a luminescent coating. In these nanoparticles, the magnetic and optical bistability of the bulk Fe-Trz polymer is preserved. Their size and shape can be easily varied by varying the Fe/Trz ratio (see the Supporting

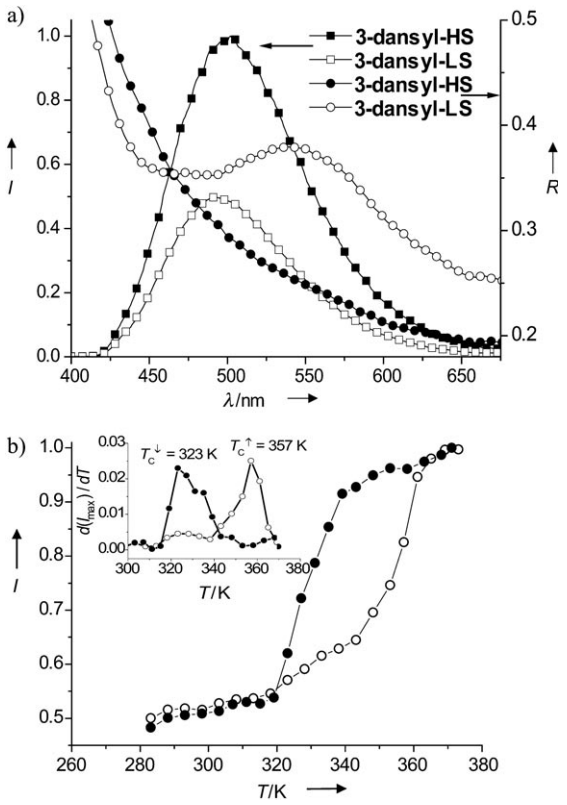

Figure 4. a) Diffuse reflectance (*R*, circles) and fluorescence (*I*, squares) spectra of **3-dansyl** measured at 280 K (LS regime, open symbols) and 400 K (HS regime, full symbols). b) Thermal variation of the fluorescence intensity at 495 nm in the heating (open circles) and cooling (filled circles) mode for **3-dansyl.**

Information), whereas the critical temperatures at which spin transition takes place can be tuned by doping the Fe-Trz complex with Zn^{II} ions. Finally, the luminescence properties of the fluorophores grafted on the surface of the SiO_2NPs⊃SCO can be adjusted by the spin state of the SCO polymer. These results clearly show that SiO_2NPs are an excellent and versatile platform to prepare new multimodal nanomaterials that may eventually exhibit a synergy between core- and shell-active components. Notice that this synergy has rarely been observed in core–shell coordination (or metal-organic coordination) structured by nanoparticles.[11] A wide number of functional molecules showing spin crossover, magnetic, superparamagnetic, or photomagnetic behavior can be immobilized within the SiO_2NPs core and their surfaces can be functionalized with different fluorophores or other nanomaterials such as quantum dots, gold, or magnetic nanoparticles. Additionally, the surface of these nanoparticles can also be functionalized with thiol, amine, or carboxy groups, which would allow the deposition of these materials on the surfaces of different substrates. We are currently studying these possibilities.

Experimental Section

1: An aqueous solution of $Fe(BF_4)_2{\cdot}6H_2O$ (211 mg, 0.625 mmol in 0.5 mL H_2O) and 0.1 mL of tetraethyl orthosilicate (TEOS) were added to a solution of Triton X-100 (1.8 mL), hexanol (1.8 mL), and cyclohexane (7.5 mL). The resulting mixture was stirred until a clear water-in-oil microemulsion had formed. A similar procedure was applied to HTrz (131 mg, 1.875 mmol) to form a second microemulsion. The two microemulsions were quickly combined and the mixture was stirred for 24 h in the dark, followed by addition of acetone to break the structure of the microemulsion and recover the particles by centrifugation. The particles were washed twice with ethanol, then with acetone, and dried at 70 °C for 12 h.

2 and **3**: Samples with two different Fe/Zn ratios (80:20 for **2** and 50:50 for **3**) were prepared by following the same method as for **1**. The concentration in water was kept constant and equal to 0.625 M, $[c(Fe^{II}) + c(Zn^{II}) = 0.625\,M]$.

Dansyl-functionalized hybrid SiO_2⊃$[Fe(HTrz)_2(Trz)]$ and SiO_2⊃-$[Fe_{1-x}Zn_x(HTrz)_2(Trz)]$ nanoparticles: The trialkoxysilane derivate 3-(dansylamido)propyltrimethoxysilane was obtained by reaction of 3-aminopropyltrimethoxysilane and dansyl chloride, following an experimental procedure described by Tonellato and co-workers.[12]

1-Dansyl: **1** (0.1 g) and 3-(dansylamido)propyltrimethoxysilane (0.025 g, 0.055 mmol) were added to a mixture of dried acetonitrile/dichloromethane (1:1, 50 mL). The resulting mixture was heated at reflux for 48 h in an inert atmosphere. The solid nanoparticles were recovered by centrifugation and washed several times with acetronitrile, ethanol, and acetone until the dansyl fluorescence had vanished in the solvent. The final solid was dried at 70 °C for 12 h.

3-Dansyl: The material was prepared following the same procedure as for **1-dansyl**, but using 0.1 g of **3** as the starting material.

Received: December 13, 2010
Published online: March 4, 2011

Keywords: luminescence · multifunctional materials · nanoparticles · silica · spin crossover

[1] "Spin Crossover in Transition Metal Compounds": *Topics in Current Chemistry* (Eds.: P. Gütlich, H. A. Goodwin), Springer, Berlin, **2004**, pp. 233 – 235.

[2] a) J. A. Real, A. B. Gaspar, V. Niel, M. C. Muñoz, *Coord. Chem. Rev.* **2003**, *236*, 121 – 141; b) P. Gütlich, A. Hauser, H. Spiering, *Angew. Chem.* **1994**, *106*, 2109 – 2141; *Angew. Chem. Int. Ed. Engl.* **1994**, *33*, 2024 – 2054; c) A. B. Gaspar, V. Ksenofontov, M. Seredyuk, P. Gütlich, *Coord. Chem. Rev.* **2005**, *249*, 2661 – 2676; d) A. Galet, A. B. Gaspar, M. C. Muñoz, G. V. Bukin, G. Levchenko, J. A. Real, *Adv. Mater.* **2005**, *17*, 2949 – 2953; e) N. Ould-Mousa, G. Mólnar, S. Bonhommeau, A. Zwick, S. Mouri, K. Tanaka, J. A. Real, A. Bousseksou, *Phys. Rev. Lett.* **2005**, *94*, 107205; f) M. Ohba, K. Yoneda, G. Agustí, M. C. Muñoz, A. B. Gaspar, J. A. Real, M. Yamasaki, H. Ando, Y. Nakao, S. Sakaki, S. Kitagawa, *Angew. Chem.* **2009**, *121*, 4861 – 4865; *Angew. Chem. Int. Ed.* **2009**, *48*, 4767 – 4771; g) S. M. Neville, G. J. Halder, K. W. Chapman, M. B. Duriska, P. D. Southon, J. D. Cashion, J. F. Létard, B. Moubaraki, K. S. Murray, C. J. Kepert, *J. Am. Chem. Soc.* **2008**, *130*, 2869 – 2876.

[3] O. Kahn, C. Jay Martinez, *Science* **1998**, *279*, 44 – 48.

[4] a) E. Coronado, J. R. Galán-Mascarós, M. Monrabal-Capilla, J. García-Martínez, P. Pardo-Ibánez, *Adv. Mater.* **2007**, *19*, 1359 – 1361; b) T. Forestier, S. Mornet, N. Daro, T. Nishihara, S. I. Mouri, K. Tanaka, O. Fouché, E. Freysz, J. F. Létard, *Chem. Commun.* **2008**, 4327 – 4329; c) F. Volatron, L. Catala, E. Rivière, A. Gloter, O. Stéphan, T. Mallah, *Inorg. Chem.* **2008**, *47*, 6584 – 6586; d) I. Boldog, A. B. Gaspar, V. Martínez, P. Pardo-Ibañez, V. Ksenofontov, A. Bhattacharjee, P. Gütlich, J. A. Real, *Angew. Chem.* **2008**, *120*, 6533 – 6537; *Angew. Chem. Int. Ed.* **2008**, *47*, 6433 – 6437; e) J. Larionova, L. Salmon, Y. Guari, A. Tokarev, K. Molvinger, G. Molnár, A. Bousseksou, *Angew. Chem.* **2008**, *120*, 8360 – 8364; *Angew. Chem. Int. Ed.* **2008**, *47*, 8236 – 8240; f) T. Forestier, A. Kaiba, S. Pechev, P. Guionneau, N. Daro, E. Freysz, J. F. Létard, *Chem. Eur. J.* **2009**, *15*, 6122 – 6130; g) V. Martínez, I. Boldog, A. B. Gaspar, V. Ksenofontov, A. Bhattacharjee, P. Gütlich, J. A. Real, *Chem. Mater.* **2010**, *22*, 4271 – 4281; h) J. R. Galán-Mascarós, E. Coronado, A. Forment-Aliaga, M. Monrabal-Capilla, E. Pinilla-Cienfuegos, M. Ceolin, *Inorg. Chem.* **2010**, *49*, 5706 – 5714.

[5] a) C. Edder, C. Piguet, J. C. Bünzli, G. Hopfgartner, *Chem. Eur. J.* **2001**, *7*, 3014 – 3024; b) H. Matsukizono, K. Kuroiwa, N. Kimizuka, *Chem. Lett.* **2008**, *37*, 446 – 447; c) M. Matsuda, H. Isozaki, H. Tajima, *Chem. Lett.* **2008**, *37*, 374 – 375.

[6] L. Salmon, G. Molnár, D. Zitouni, C. Quintero, C. Bergaud, J. C. Micheau, A. Bousseksou, *J. Mater. Chem.* **2010**, *20*, 5499 – 5503.

[7] a) A. Burns, H. Ow, U. Wiesner, *Chem. Soc. Rev.* **2006**, *35*, 1028 – 1042; b) W. Tan, K. Wang, X. He, X. J. Zhao, T. Drake, L. Wang, R. P. Bagwe, *Med. Res. Rev.* **2004**, *24*, 621 – 638; c) L. Wang, K. Wang, S. Santra, X. Zhao, L. R. Hilliard, J. Smith, Y. Wu, W. Tan, *Anal. Chem.* **2006**, *78*, 646 – 654; d) A. B. Descalzo, R. Martínez-Máñez, F. Sancenón, K. Hoffmann, K Rurack, *Angew. Chem.* **2006**, *118*, 6068 – 6093; *Angew. Chem. Int. Ed.* **2006**, *45*, 5924 – 5948; e) Y. Jin, A. Li, S. G. Hazelton, S. Liang, C. L. John, P. D. Selid, D. T. Pierce, J. X. Zhao, *Coord. Chem. Rev.* **2009**, *253*, 2998 – 3014.

[8] J. Kroeber, J. P. Audière, R. Claude, E. Codjovi, O. Kahn, J. G. Haasnoot, F. Grolière, C. Jay, A. Bousseksou, J. Linares, F. Varret, A. Gonthier-Vassal, *Chem. Mater.* **1994**, *6*, 1404 – 1412.

[9] a) F. Arriagada, K. Osseo-Asare, *Colloids Surf.* **1999**, *154*, 311 – 326; b) R. P. Bagwe, C. Yang, L. R. Hilliard, W. Tan, *Langmuir* **2004**, *20*, 8336 – 8342.

[10] a) M. Montalti, L. Prodi, N. Zaccheroni, G. Falini, *J. Am. Chem. Soc.* **2002**, *124*, 13540 – 13546; b) L. Mu, W. Shi, G. She, J. C. Chang, S. T. Lee, *Angew. Chem.* **2009**, *121*, 3521 – 3524; *Angew. Chem. Int. Ed.* **2009**, *48*, 3469 – 3472.

[11] L. Catala, D. Brinzei, Y. Prado, A. Gloter, O. Stéphan, G. Rogez, T. Mallah, *Angew. Chem.* **2009**, *121*, 189 – 193; *Angew. Chem. Int. Ed.* **2009**, *48*, 183 – 187.

[12] E. Brasola, F. Mancin, E. Rampazzo, P. Tecilla, U. Tonellato, *Chem. Commun.* **2003**, 3026 – 3027.

